

# Expulsion of Ions from Hydrophobic Hydration Shells

Blake M. Rankin and Dor Ben-Amotz\*

Department of Chemistry, Purdue University, 560 Oval Drive, West Lafayette, Indiana 47906, United States

**S** Supporting Information

**ABSTRACT:** Raman spectroscopy is combined with multivariate curve resolution to quantify interactions between ions and molecular hydrophobic groups in water. The molecular solutes in this study all have similar structures, with a trimethyl hydrophobic domain and a polar or charged headgroup. Our results imply that aqueous sodium and fluoride ions are strongly expelled from the first hydration shells of the hydrophobic (methyl) groups, while iodide ions are found to enter the hydrophobic hydration shell, to an extent that depends on the methyl group partial charge. However, our quantitative estimates of the corresponding ion binding equilibrium constants indicate that the iodide concentration in the first hydrophobic hydration shell is generally lower than that in the surrounding bulk water, and so an iodide ion cannot be viewed as having a true affinity for the molecular hydrophobic interface, but rather is less strongly expelled from such an interface than fluoride.

The affinity of ions for molecular interfaces is of wide-ranging importance in chemistry, geology, and biology, including the role of ions in protein folding and stability.<sup>1</sup> The Hofmeister series has been used to quantify and categorize specific ion interactions and their biological relevance.<sup>1–4</sup> For example, the adsorption of ions to macroscopic air–water and oil–water interfaces has been investigated using experimental thermodynamic analyses,<sup>5</sup> interfacial tension,<sup>6</sup> nonlinear optical second harmonic generation,<sup>7,8</sup> sum frequency experiments,<sup>9–12</sup> and X-ray photoelectron spectroscopy.<sup>13</sup> While both MD simulations and thermodynamic analyses indicate that Na<sup>+</sup> and F<sup>−</sup> are expelled from macroscopic air–water and molecular hydrophobic interfaces, some previous studies have suggested that large polarizable anions have an affinity for macroscopic air–water and oil–water interfaces and molecular hydrophobic hydration shells.<sup>2,5,10,12,14–19</sup> Our recent combined experimental and theoretical study has confirmed that I<sup>−</sup> ions enter the first hydration shell of *tert*-butyl alcohol (TBA), while Na<sup>+</sup> and F<sup>−</sup> ions do not.<sup>20</sup> Here we extend the latter results to include a series of solutes that resemble TBA in shape but have different head groups, in order to quantify the influence of interfacial charge and neighboring polar groups on the affinity of ions for molecular hydrophobic hydration shells.

Despite the significant number of computer simulation studies of ions at aqueous interfaces,<sup>15</sup> including the affinities of alkali cations and halide anions for lipid membranes<sup>21</sup> and peptide bonds,<sup>22</sup> few previous experiments have confirmed the presence of large ions in the *first* hydration layer of hydrophobic interfaces. The only exceptions (to the best of

our knowledge) include our recent study<sup>20</sup> and a recent NMR and MD study which concluded that, while I<sup>−</sup> and SCN<sup>−</sup> bind to the amide groups and CH<sub>2</sub> backbone of an uncharged polypeptide, (VPGVG)<sub>120</sub>, they do not interact with the hydrophobic side chains.<sup>23</sup> Furthermore, a combined NMR and isothermal titration calorimetry study found that I<sup>−</sup> and other chaotropic ions bind to a concave aromatic hydrophobic cavity.<sup>24</sup>

To gain a better fundamental understanding of the effect of headgroup charge and polarity on the affinity of ions for hydrophobic hydration shells, we have applied Raman multivariate curve resolution (MCR) hydration shell spectroscopy<sup>20,25</sup> to probe the affinity of Na<sup>+</sup>, F<sup>−</sup>, and I<sup>−</sup> for the hydrophobic surfaces of a class of amphiphilic solutes of similar shape: trimethylacetate (TMA<sup>−</sup>), *tert*-butylamine (TBNH<sub>2</sub>), TBA, trimethylamine *N*-oxide (TMAO), and tetramethylammonium (TMeA<sup>+</sup>), as shown in Figure 3B. Note that the positive charge of TMeA<sup>+</sup> is expected to delocalize over the methyl groups,<sup>26</sup> and TMAO is a zwitterionic osmolyte with a dipole moment oriented toward the oxygen atom, and thus its methyl groups are also expected to have a partial positive charge.<sup>27</sup> We refer to methyl groups as nominally hydrophobic because neopentane, C(CH<sub>3</sub>)<sub>4</sub>, is insoluble in water, and thus the high aqueous solubility of the above solutes may be attributed to their polar head groups (or net charge). We have obtained quantitative information regarding the affinity of various ions for the hydrophobic domain of these solutes by using self-modeling curve resolution (SMCR)<sup>28</sup> to detect ion-induced CH (or CD) frequency shifts and quantify the probability that a given ion will reside within the first hydration shell of each of the above solutes. Moreover, observed perturbations of the hydrophobic hydration shell structure provide further evidence of interactions between ions and hydrophobic groups. We have also performed atomic partial charge calculations to quantify the correlation between surface charge and ion affinity.

Figure 1A shows the solute-correlated (SC) spectra obtained from a 0.5 M solution of TMAO in water containing various concentrations of NaF (up to 1 M). These SC spectra reveal the CH stretch band of TMAO (between ~2800 and 3100 cm<sup>−1</sup>), as well as features arising from hydration shell water molecules (between ~3100 and 3700 cm<sup>−1</sup>) whose vibrational structure is perturbed by the solute. The low-frequency shoulder of the hydration shell OH band near 3200 cm<sup>−1</sup> (Figure 1A) implies that the tetrahedral structure of water is enhanced around TMAO.<sup>20,25,29–31</sup> More significantly, the insensitivity of the TMAO hydration shell spectrum to added

Received: April 11, 2013

Published: June 4, 2013

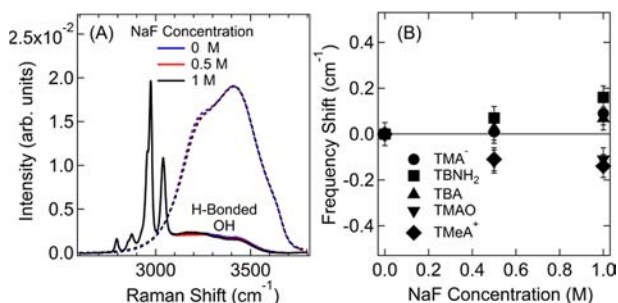


**Figure 1.** (A) SC spectra of TMAO in aqueous solutions of NaF. The dashed curves correspond to the solvent component (pure water or aqueous NaF). (B) Neither Na<sup>+</sup> nor F<sup>-</sup> induces a significant shift in the CH frequencies of TMA<sup>-</sup>, TBNH<sub>2</sub>, TBA, or TMeA<sup>+</sup>. The NaF concentration is that of the aqueous salt solution, before the molecular solute was added.

NaF indicates that the hydration shell of TMAO is not disrupted by either Na<sup>+</sup> or F<sup>-</sup> ions. Furthermore, the results shown in Figure 1B indicate that aqueous NaF has little or no effect on the CH stretching frequency of TMAO or the other molecular solutes, including the positively charged TMeA<sup>+</sup>. These results imply that both Na<sup>+</sup> and F<sup>-</sup> are expelled from the hydration shells of all these solutes.

Since both Na<sup>+</sup> and F<sup>-</sup> are expelled from the hydration shell of TMAO, any changes in the SC spectra of TMAO in aqueous NaI can be attributed to the specific interactions between I<sup>-</sup> and its hydrophobic trimethyl domain. The results displayed in Figure 2A indicate that I<sup>-</sup> does indeed disrupt the hydration

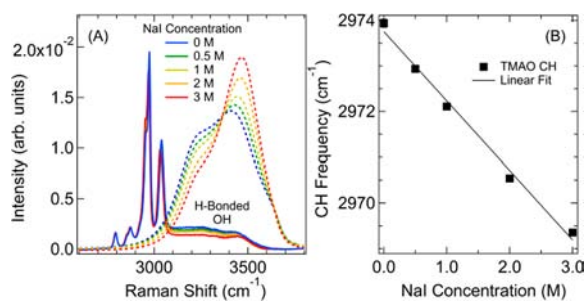


**Figure 2.** (A) SC spectra of TMAO in aqueous solutions of NaI. The dashed curves correspond to the solvent component (pure water or aqueous NaI). (B) I<sup>-</sup> induces a 1.54 cm<sup>-1</sup>/M NaI red-shift in the CH frequency with increasing I<sup>-</sup> concentration. The NaI concentration is that before the molecular solute was added.

shell of TMAO, as evidenced by the decrease in the SC OH band intensity near ~3200 cm<sup>-1</sup>. Furthermore, I<sup>-</sup> induced a significant red-shift in the CH stretch of TMAO with a slope of ~1.54 cm<sup>-1</sup>/M (Figure 2B).

The fact that the CH frequency shift in Figure 2B is approximately linear implies that I<sup>-</sup> has little affinity for the hydrophobic surface of TMAO—as a strong affinity would result in a nonlinear concentration dependence (as further discussed below, and illustrated in Figure 5). Moreover, previous comparisons of experimental and theoretical results for TBA in aqueous NaI imply that CH shifts of this magnitude arise from the I<sup>-</sup> ions in the first hydration shell of the methyl groups (rather than second or higher hydration shells).<sup>20</sup>

Figure 3A shows how the CH frequencies of TMA<sup>-</sup>, TBNH<sub>2</sub>, TBA, TMAO, and TMeA<sup>+</sup> shift as a function of I<sup>-</sup> concentration. The largest I<sup>-</sup>-induced CH red-shift of ~3

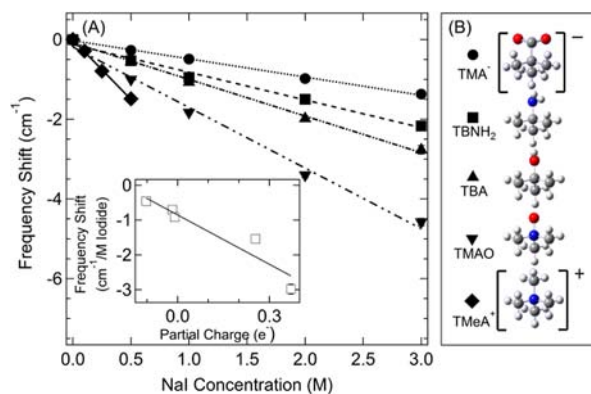


**Figure 3.** (A) I<sup>-</sup>-induced CH frequency shifts of TMA<sup>-</sup>, TBNH<sub>2</sub>, TBA, TMAO, and TMeA<sup>+</sup> as a function of I<sup>-</sup> concentration (and best-fit lines). The inset shows the solute CH frequency shift plotted as a function of the methyl group partial charge (along with a best-fit line of slope -4.7 cm<sup>-1</sup> M<sup>-1</sup> e<sup>-1</sup>). (B) Solute structures (and symbols). The concentrations of the molecular solutes are all 0.5 M, except TMeA<sup>+</sup> which is 0.1 M.

cm<sup>-1</sup>/M NaI was found for TMeA<sup>+</sup>, suggesting that I<sup>-</sup> interacts more strongly with this positively charged solute than with TMAO. Further analysis (described below) indicates that the different slopes in Figure 3A reflect the different probabilities of finding a single I<sup>-</sup> ion in the first hydration shell of each of the above solutes.

To gain further insight into the electrostatic contributions to interactions between I<sup>-</sup> and the methyl groups on solutes with different head groups and charge, we have performed atomic partial charge calculations on each of the isolated solutes (see Supporting Information (SI) for further details). Although the absolute values of these charges depend on the method and level of theory used, all of our results suggest that the methyl groups on TMeA<sup>+</sup> are more positively charged than the methyl groups on TMAO. Moreover, the inset in Figure 3A shows that the observed I<sup>-</sup>-induced CH frequency shifts increase with increasing methyl group (positive) charge (see also Table S1).

We have also used Raman-MCR to obtain ion-correlated (rather than molecular solute-correlated) spectra that contain additional quantitative information regarding interactions between I<sup>-</sup> and hydrophobic hydration shells. The following procedure is similar to that used previously,<sup>20</sup> but modified to yield a more self-consistent estimate of the number of molecular solutes whose hydration shells contain I<sup>-</sup>. First of all, in order to eliminate the overlap between the OH stretch of water and the CH stretch of the solute, experiments were performed using a solvent consisting of a 0.5 M aqueous solution of either deuterated TBA (TBA-d<sub>9</sub>) or TMAO (TMAO-d<sub>9</sub>). Various concentrations of NaI were added to these two-component solvents, and SMCR was used to decompose the resulting experimental spectra into I<sup>-</sup>-correlated and pure solvent spectral contributions. The resulting I<sup>-</sup>-correlated spectra contain features arising from any molecular solutes (TBA or TMAO) whose spectra are significantly perturbed by I<sup>-</sup>. In other words, any TBA or TMAO molecules whose first hydration shells contain I<sup>-</sup> are expected to appear in the I<sup>-</sup>-correlated spectrum, while those TBA or TMAO molecules whose hydration shells do not contain I<sup>-</sup> will show up in the solvent spectrum (pertaining to salt-free aqueous TBA or TMAO).

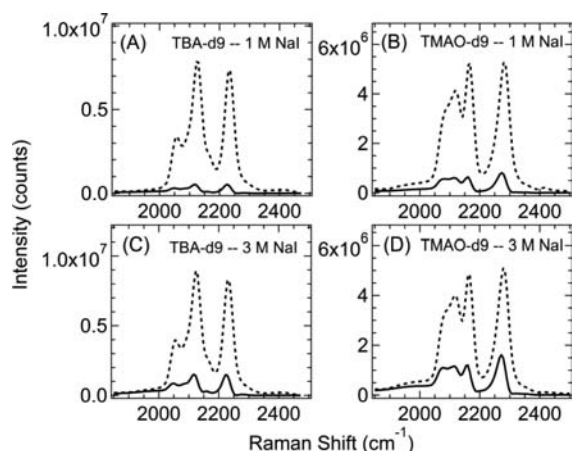


**Figure 4.** Expanded CD peaks of 1 M (A,B) and 3 M (C,D)  $I^-$ -correlated spectra in an aqueous solvent containing TBA- $d_9$  (A,C) and TMAO- $d_9$  (B,D). The dashed curves represent the input Raman spectra, and the solid curves represent the  $I^-$ -correlated component pertaining to solutes whose methyl groups are perturbed by  $I^-$ .

Figure 4 displays the CD stretch bands appearing in the  $I^-$ -correlated spectra obtained when either 1 M or 3 M NaI is added to aqueous TBA- $d_9$  and TMAO- $d_9$  solvents. The dashed curves represent the CD stretch band in the input Raman spectra. The solid curves represent the  $I^-$ -correlated CD band arising from TBA or TMAO molecules whose hydration shell contains an  $I^-$  ion. Note that the areas under the solid curves, and thus the number of perturbed TBA or TMAO molecules, increase approximately linearly with  $I^-$  concentration. However, the CD red-shift (relative to that of the solute in salt-free water) is remarkably independent of salt concentration (as further described below). A similar analysis of 1 M NaF in aqueous TBA- $d_9$  and TMAO- $d_9$  reveals no  $F^-$ -correlated CD features, confirming that there are no  $F^-$  ions in the first hydration shells of TBA or TMAO (see SI).

The above procedure was extended to solvents containing non-deuterated TMA $^-$ , TBNH $_2$ , TBA, TMAO, and TMeA $^+$  using a two-step SMCR analysis procedure (as further described in SI). The resulting  $I^-$ -induced CH and CD frequency shifts obtained from the corresponding  $I^-$ -correlated spectra were all found to be quite similar,  $9 \pm 3 \text{ cm}^{-1}$ . The fact that the magnitude of these shifts is independent of  $I^-$  concentration (while the area of the perturbed CH or CD band scales with  $I^-$  concentration) implies that the different CH frequency shift slopes shown in Figure 3A reflect the different probabilities that a single  $I^-$  ion will be found in the corresponding hydrophobic hydration shells (as further discussed in the SI).

Results such as those shown in Figure 4 may be used to determine the ratio of the perturbed ( $I^-$ -correlated) CD band area to the total CD band area in the input mixture spectrum, and thus obtain a quantitative estimate of the fraction,  $f$ , of molecules whose first hydration shells contain  $I^-$ .

$$f = \frac{[SI^-]}{[SI^-] + [S]} \approx \frac{A_{SI^-}}{A_{SI^-} + A_S} \quad (1)$$

where  $[SI^-]$  and  $[S]$  are the concentrations of the molecular solutes whose first hydration shells either do or do not contain  $I^-$ , respectively, and  $A_{SI^-}$  and  $A_S$  are the corresponding CD band areas. Moreover, we may use the resulting  $f$  values to estimate

the equilibrium constants pertaining to a simple ion–molecule association process of the form  $S_{aq} + I_{aq}^- \rightleftharpoons SI_{aq}^-$ :

$$K_A = \frac{[SI^-]}{[S][I^-]} = \frac{f[S]_0}{([S]_0 - f[S]_0)([I^-]_0 - f[S]_0)} \quad (2)$$

Note that  $[S]_0 = [SI^-] + [S]$  and  $[I^-]_0 = [SI^-] + [I^-]$  are the total concentrations of the molecular solute and iodide ion, respectively. If there were a true affinity between  $I^-$  ions and the molecular solute, then we would expect to observe a large equilibrium constant  $K_A > 1 \text{ M}^{-1}$  (and  $\Delta G < 0$ ), while a small equilibrium constant  $K_A < 1 \text{ M}^{-1}$  (and  $\Delta G > 0$ ) would indicate that  $I^-$  ions are expelled from the molecular hydration shell. The cutoff value of  $K_A \approx 1 \text{ M}^{-1}$  is similar to that estimated assuming a random mixture in which the  $I^-$  concentration in the molecular hydration shell is the same as that of the surrounding solvent (as further discussed in the SI). The results shown in Figure 4 indicate that  $K_A \approx 0.07 \pm 0.01$  and  $0.21 \pm 0.08 \text{ M}^{-1}$  for TBA and TMAO, respectively, thus implying that  $I^-$  is expelled from the first hydration shells of both these solutes, but less so from TMAO than TBA.

Figure 5 compares predictions obtained using eq 2 (curves) assuming  $K_A = 0.1, 1$ , and  $10 \text{ M}^{-1}$ , with experimentally derived

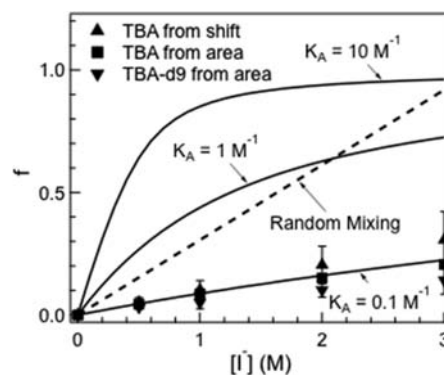


**Figure 5.** Predicted values of  $f$  assuming that  $K_A = 0.1, 1$ , and  $10 \text{ M}^{-1}$ . The points are experimentally derived  $f$  values obtained using three different methods (see text for details).

values of  $f$  (points) for TBA and TBA- $d_9$ , obtained either from ion-correlated band areas (such as those in Figure 4) or from solute CH or CD frequency shifts (as described below). Although there is significant scatter in the experimentally derived  $f$  values, these results clearly confirm that  $K_A \approx 0.1 \text{ M}^{-1}$  for TBA. The dashed curve in Figure 5 shows random mixing predictions obtained assuming that the local iodide concentration is equal to that in the surrounding solution. The linear concentration dependence of the experimental  $f$  values, as well as the fact that they lie well below the random mixing predictions, again confirms that  $I^-$  is expelled from the first hydration shell of TBA (and results obtained for the other molecular solutes are shown in Figure S4).

Our conclusion that  $I^-$  is expelled from the first hydration shells of TBA and TMAO is quite robust, as similar results are obtained using both deuterated and non-deuterated TBA and TMAO (see SI), as well as using the following alternative procedure. Since our  $I^-$ -correlated spectra indicate that an  $I^-$  anion within the hydrophobic hydration shell produces a CH shift of  $9 \pm 3 \text{ cm}^{-1}$ , we may use the concentration-dependent shifts shown in Figure 3A to estimate  $f$  and thus also  $K_A$ . For example, Figure 3A indicates that when  $[NaI] = 1 \text{ M}$  the

average CH stretch of TMAO is red-shifted by  $1.54\text{ cm}^{-1}$ , which, when combined with the above  $9 \pm 3\text{ cm}^{-1}$  shift per  $\Gamma^-$ , implies that between 13% and 26% of the TMAO molecules contain an  $\Gamma^-$  in their first hydration shell. The latter percentages correspond to  $K_A \approx 0.23 \pm 0.12\text{ M}^{-1}$ , and the  $K_A$  values obtained in a similar way for the other molecular solutes range from  $K_A \approx 0.06 \pm 0.02\text{ M}^{-1}$  for  $\text{TMA}^-$  to  $K_A \approx 0.41 \pm 0.20\text{ M}^{-1}$  for  $\text{TMeA}^+$ . Although  $K_A < 1\text{ M}^{-1}$  for all these solutes, the  $\text{TMeA}^+$  results are quite close to those pertaining to a random mixture (see SI).

Somewhat higher estimates of  $K_A$  may be obtained by considering the mathematical rotational ambiguity inherent in MCR,<sup>31</sup> which implies that  $9\text{ cm}^{-1}$  may be an upper bound to the true CH red-shift induced by a single first hydration shell  $\Gamma^-$  ion (and that the area of the corresponding  $\Gamma^-$ -correlated CH or CD band may be a lower bound to the true band area). However, our qualitative conclusions would not significantly change even if we decreased the  $9\text{ cm}^{-1}$  CH or CD shift to  $4\text{ cm}^{-1}$ , in keeping with the CH red-shift predicted using hybrid quantum-classical calculations for aqueous TBA whose first hydration shell contains a single  $\Gamma^-$  ion.<sup>20</sup> More specifically, assuming a  $4\text{ cm}^{-1}$  red-shift would increase our derived  $K_A$  values by about a factor of 2, and thus would imply that the concentration of  $\Gamma^-$  in the first hydration shell of TMAO may be close to that in a random mixture, and the  $\Gamma^-$  concentration around  $\text{TMeA}^+$  may slightly exceed that in the surrounding solution (see Table S2 and the associated discussion in the SI).

In summary, we have used Raman-MCR to quantitatively compare the affinity of  $\text{F}^-$  and  $\Gamma^-$  ions for the hydration shells of solutes containing methyl groups of different partial charge. Our results imply that the local anion concentrations in the first hydration shell increase with increasing methyl group (positive) charge and with increasing anion size, but typically remain lower than that in the surrounding solution. The most extreme case is that of the cationic solute  $\text{TMeA}^+$ , for which our results indicate that the local  $\Gamma^-$  concentration may slightly exceed that in the surrounding solution. Our results are in general agreement with previous MD simulations and thermodynamic analyses of ion partitioning at air–water interfaces and molecular hydrophobic hydration shells,<sup>2,5,10,12,14–19</sup> although we find that  $\Gamma^-$  has a somewhat lower affinity for hydrophobic hydration shells than previously implied.

## ■ ASSOCIATED CONTENT

### ● Supporting Information

Experimental and theoretical methods and supplementary results. This material is available free of charge via the Internet at <http://pubs.acs.org>.

## ■ AUTHOR INFORMATION

### Corresponding Author

bendor@purdue.edu

### Notes

The authors declare no competing financial interest.

## ■ ACKNOWLEDGMENTS

This work was funded by NSF (CHE-1213338) and a PRF Research Grant from Purdue University. The authors acknowledge Lyudmila V. Slipchenko for suggestions regarding the calculation of atomic partial charges.

## ■ REFERENCES

- (1) Collins, K. D. *Methods* **2004**, *34*, 300.
- (2) Pegram, L. M.; Record, M. T. *J. Phys. Chem. B* **2008**, *112*, 9428.
- (3) Zhang, Y.; Cremer, P. S. *Annu. Rev. Phys. Chem.* **2010**, *61*, 63.
- (4) Lo Nostro, P.; Ninham, B. W. *Chem. Rev.* **2012**, *112*, 2286.
- (5) Pegram, L. M.; Record, M. T. *J. Phys. Chem. B* **2007**, *111*, 5411.
- (6) dos Santos, A. P.; Levin, Y. *Langmuir* **2012**, *28*, 1304.
- (7) Onorato, R. M.; Otten, D. E.; Saykally, R. J. *Proc. Natl. Acad. Sci. U.S.A.* **2009**, *106*, 15176.
- (8) Onorato, R. M.; Otten, D. E.; Saykally, R. J. *J. Phys. Chem. C* **2010**, *114*, 13746.
- (9) McFearin, C. L.; Richmond, G. L. *J. Phys. Chem. C* **2009**, *113*, 21162.
- (10) Jubb, A. M.; Hua, W.; Allen, H. C. *Acc. Chem. Res.* **2012**, *45*, 110.
- (11) Flores, S. C.; Kherb, J.; Konelick, N.; Chen, X.; Cremer, P. S. *J. Phys. Chem. C* **2012**, *116*, 5730.
- (12) Liu, D.; Ma, G.; Levering, L. M.; Allen, H. C. *J. Phys. Chem. B* **2004**, *108*, 2252.
- (13) Ghosal, S.; Hemminger, J. C.; Bluhm, H.; Mun, B. S.; Hebenstreit, E. L. D.; Ketteler, G.; Ogletree, D. F.; Requejo, F. G.; Salmeron, M. *Science* **2005**, *307*, 563.
- (14) Dang, L. X.; Chang, T. M. *J. Phys. Chem. B* **2002**, *106*, 235.
- (15) Jungwirth, P.; Tobias, D. J. *Chem. Rev.* **2005**, *106*, 1259.
- (16) Vazdar, M.; Pluharova, E.; Mason, P. E.; Vacha, R.; Jungwirth, P. *J. Phys. Chem. Lett.* **2012**, *3*, 2087.
- (17) Baer, M. D.; Mundy, C. J. *J. Phys. Chem. Lett.* **2011**, *2*, 1088.
- (18) Netz, R. R.; Horinek, D. *Annu. Rev. Phys. Chem.* **2012**, *63*, 401.
- (19) Vaikuntanathan, S.; Shaffer, P. R.; Geissler, P. L. *Faraday Discuss.* **2013**, *160*, 63.
- (20) Rankin, B. M.; Hands, M. D.; Wilcox, D. S.; Fega, K. R.; Slipchenko, L. V.; Ben-Amotz, D. *Faraday Discuss.* **2013**, *160*, 255.
- (21) Vacha, R.; Siu, S. W. I.; Petrov, M.; Bockmann, R. A.; Barucha-Kraszewska, J.; Jurkiewicz, P.; Hof, M.; Berkowitz, M. L.; Jungwirth, P. *J. Phys. Chem. A* **2009**, *113*, 7235.
- (22) Heyda, J.; Vincent, J. C.; Tobias, D. J.; Dzubiella, J.; Jungwirth, P. *J. Phys. Chem. B* **2010**, *114*, 1213.
- (23) Rembert, K. B.; Paterova, J.; Heyda, J.; Hilty, C.; Jungwirth, P.; Cremer, P. S. *J. Am. Chem. Soc.* **2012**, *134*, 10039.
- (24) Gibb, C. L. D.; Gibb, B. C. *J. Am. Chem. Soc.* **2011**, *133*, 7344.
- (25) Davis, J. G.; Gierszal, K. P.; Wang, P.; Ben-Amotz, D. *Nature* **2012**, *491*, 582.
- (26) Luzhkov, V. B.; Sterberg, F.; Acharya, P.; Chattopadhyaya, J.; Qvist, J. *J. Phys. Chem. Chem. Phys.* **2002**, *4*, 4640.
- (27) Sagle, L. B.; Cimatu, K.; Litosh, V. A.; Liu, Y.; Flores, S. C.; Chen, X.; Yu, B.; Cremer, P. S. *J. Am. Chem. Soc.* **2011**, *133*, 18707.
- (28) Lawton, W. H.; Sylvestre, E. A. *Technometrics* **1971**, *13*, 617.
- (29) Torii, H. *J. Phys. Chem. A* **2006**, *110*, 9469.
- (30) Auer, B. M.; Skinner, J. L. *Chem. Phys. Lett.* **2009**, *470*, 13.
- (31) Yang, M.; Skinner, J. L. *J. Phys. Chem. Chem. Phys.* **2010**, *12*, 982.